

Supplementary data for article:

Lama, S. M. G.; Pampel, J.; Fellingner, T.-P.; Beškoski, V. P.; Slavković-Beškoski, L.; Antonietti, M.; Molinari, V. Efficiency of Ni Nanoparticles Supported on Hierarchical Porous Nitrogen-Doped Carbon for Hydrogenolysis of Kraft Lignin in Flow and Batch Systems. *ACS Sustainable Chemistry and Engineering* **2017**, 5 (3), 2415–2420.

<https://doi.org/10.1021/acssuschemeng.6b02761>

Electronic Supplementary Information

Efficiency of Ni-nanoparticles supported on a hierarchical porous nitrogen doped carbon for the hydrogenolysis of Kraft lignin in flow and batch systems

Sandy M. G. Lama^a, Jonas Pampel^a, Tim-Patrick Fellingner^a, Vladimir P. Beškosi^b, Latinka Slavković-Beškosi^c, Markus Antonietti^a, Valerio Molinari^{a*}

^a*Max Planck Institute of Colloids and Interfaces, Am Mühlenberg 1, 14424 Potsdam, Germany.*

E-mail: Valerio.Molinari@mpikg.mpg.de

^b*University of Belgrade, Faculty of Chemistry, Studentski trg 12-16, P.O.Box 158, 11001 Belgrade, Serbia*

^c*University of Belgrade, Institute of Nuclear Sciences "Vinča", Mike Petrovića Alasa 12-14, P.O. Box 522, 11001 Belgrade, Serbia*

Total number of pages: 26 (S1–S26) including 17 Figures and 6 Tables

List of Figures

Figure S 1 SEM image of NDC support	5
Figure S 2 EDX images of NDC support unwashed (A) and washed (B) from the iron impurities.....	5
Figure S 3 These SEM images show the changes that occur to the Ni-NDC catalyst under different temperatures (A: 300 °C, B: 400 °C, C: 500 °C at which the high temperature effect starts, and D: 600 °C).....	6
Figure S 4 SEM and EDX mapping on Ni-NDC composite	7
Figure S 5 XRD of Ni- composites before reactions	7
Figure S 6 Particle size distribution observed by several TEM images	8
Figure S 7 XRD of Ni-NDC before reaction (Fresh), recovered from flow reaction of 100 hrs (Flow), and recovered from batch reaction of 24 hrs (Batch).	18
Figure S 8 XRD of Ni-C before reaction (Fresh), recovered from flow reaction of 25 hrs (Flow), and recovered from batch reaction of 24 hrs (Batch).....	18
Figure S 9 XRD of Ni-C _{ref} before reaction (Fresh) and after being recovered from batch reaction of 24 hrs (Batch). ..	19
Figure S 10 X-ray photoelectron spectroscopy of Ni _{2p3/2} bonds in the three catalytic systems (Ni-NDC, Ni-C and Ni-Vulcan).	21
Figure S 11 X-ray photoelectron spectroscopy deconvolution curves of N _{1s} bonds in NDC and Ni-NDC	22
Figure S 12 2D-NMR of Kraft Lignin.....	23
Figure S 13 2D-NMR of Kraft Lignin after flow reaction catalyzed by Ni-NDC	23
Figure S 14 2D-NMR of Kraft Lignin after batch reaction catalyzed by Ni-NDC	24
Figure S 15 2D-NMR of Kraft Lignin after batch reaction catalyzed by Ni-C	24
Figure S 16 2D-NMR of Kraft Lignin after batch reaction catalyzed by Ni-C _{ref}	25
Figure S 17 GC-FID chromatograms of degraded lignin after 24 and 50 hours using Ni-NDC in the flow system	26

List of Tables

Table S 1 Elemental content in wt. % of Fe detected by SEM-EDX	5
Table S 2 Several properties of the different fresh Ni-C composites	8
Table S 3 Compounds detected by GCxGC-MS in depolymerized lignin samples.	9
Table S 4 ICP results of Ni content (mg/kg) in the products and the catalyst	17
Table S 5 several properties of Ni-C composites after Flow and Batch reactions	20
Table S 6 Elemental Analysis of the components of Ni-NDC under different reaction conditions.....	26

Materials

Nickel (II) Nitrate hexahydrate, heptane and Ethanol were purchased from Sigma Aldrich and used as received. Kraft lignin purchased from UPM BioPiva™ in Europe, commercial Carbon, D-glucosamine hydrochloride and zinc chloride of $\geq 98\%$ were purchased from Alfa Aesar, potassium chloride $>99.5\%$ was purchased from Roth, and medium size empty cartridges were purchased from ThalesNano use to pack the different catalysts in.

Methods

For comprehensive two dimensional gas chromatography – mass spectrometry (GC×GC-MS) analysis, degraded lignin samples were dissolved in dichloromethane and subjected to sonication for 15 minutes. The suspensions were filtered (membrane filter 0.45 μm , Agilent) and sample solutions were analyzed using GC×GC-MS gas chromatograph-quadrupole mass spectrometer GCMS-QP2010 Ultra (Shimadzu, Kyoto, Japan) and ZX2 thermal modulation system (Zoex Corp.) as Total Ion Chromatograms (TIC). A Rtx®-1 (first column: RESTEK, Crossbond® 100% dimethyl polysiloxane, 30 m, 0.25 mm ID, $d_f=0.25\ \mu\text{m}$) and a BPX50 (SGE Analytical Science, 1 m, 0.1 mm ID, $d_f=0.1\ \mu\text{m}$) column were connected through the GC×GC modulator as the first and second capillary columns, respectively. The temperature program started with an isothermal step at 40 °C for 5 min. Next, the temperature was increased from 40 to 300 °C by 5.2 °C min^{-1} . The program finished with an isothermal step at 300 °C for 5 min. The modulation applied for the comprehensive GC×GC analysis was a hot jet pulse (400 ms) every 9000 ms. The MS data was collected with Shimadzu GC/MS Real Time Analysis. The GC×GC-MS data were analyzed using ChromeSquare 2.1 software, which is capable of directly reading GC×GC data obtained with GC-MS solution, converting it to a 2-dimensional image. The degradation products were identified by a search of the MS spectrum with the MS libraries NIST 11, NIST 11s, and Wiley 8.

The X-ray diffraction measurements (XRD) are equipped with a Bruker D8 diffractometer with Cu-K α source ($\lambda = 0.154\ \text{nm}$) and a scintillation counter. The reference patterns are found in the ICDD PDF-4+ database (2014 edition). For the TEM images a Zeiss EM 912 Ω microscope was used at an acceleration voltage of 120 kV. The SEM device used has a LEO 1550 Gemini microscope. The N₂ gas sorption applied for the experiments used a Quantachrome Quadrasorb apparatus. Before starting the analysis of each sample a degassing took place (150 °C, 20 hours), then the results analysis was via QuadraWin software (version 5.05). The pore size distribution was calculated applying the QSDFT model equilibrium. The Elemental analysis used a combustion analysis of a Vario Micro device. 2D-NMR HSQC spectra were obtained through an Agilent 400 MHz Spectrometer in deuterated solvents. The Size exclusion chromatography (GPC/SEC) with UV/RI detection performed via N-methyl-2-pyrrolidone as eluent at 70°C using two PSS-GRAM columns (300 mm, 8 mm²). The average particle size used was of 7 μm and the porosity measured between 100–1000 Å. The Standard for the calibration was Polystyrene. Conversions and yields for lignin reaction were calculated by mass difference after liquid chromatographic separation. The GC-FID analysis was performed using an Agilent Technologies 5975 gas chromatograph equipped with an FID detector combined with a second HP-5MS capillary column. The temperature program for degraded lignin was set with an isothermal step to start at 50 °C for 2 min then the temperature would increase to 300 °C at a rate of 10 °C/min kept till 20 min, where the temperature of the detector is kept at 280 °C.

The evaluation of small molecular weight molecules concentration, yielded after lignin degradation, was achieved with GC-FID measurements. The integration of the signals derived from lignin derived products were compared to an internal standard (heptane).

Synthesis of NDC support

130 g of D-glucosamine hydrochloride ($\geq 98\%$, Alfa Aesar) was ball milled with the 124 g of potassium chloride ($> 99.5\%$, Roth) and the 266 g zinc chloride (98% , Alfa Aesar) representing the eutectic KCl/ZnCl₂ ratio. The obtained white powder was transferred to a ceramic boule and heated in a pottery kiln (Rohde) under nitrogen atmosphere. The heating rate was set to 2.5 K min^{-1} , the final temperature to $900\text{ }^\circ\text{C}$ and the final holding time to 1 h. After cooling to room temperature the black, monolithic structure was grinded, washed with large excess of deionized water (until the change in conductivity of the deionized water was negligible) and dried in vacuum at $60\text{ }^\circ\text{C}$ for 48 hours. Later, the mixture was washed with 1M HCl to remove any Fe residuals.

Synthesis of Ni- composites via incipient wet impregnation

232 mg of the precursor Nickel nitrate hexahydrate was dissolved in 0.8 ml distilled water and was impregnated on 100 mg of carbon support (32wt.% Ni deposited) dropwise. The mixture is air dried overnight prior to heating it under Ar/H₂ pressure up to $450\text{ }^\circ\text{C}$ in a rate of $3\text{ }^\circ\text{C/min}$ for 3 hrs then cooled down in a rate of $5\text{ }^\circ\text{C/min}$. This catalyst was prepared at different temperatures yet at the same rate.

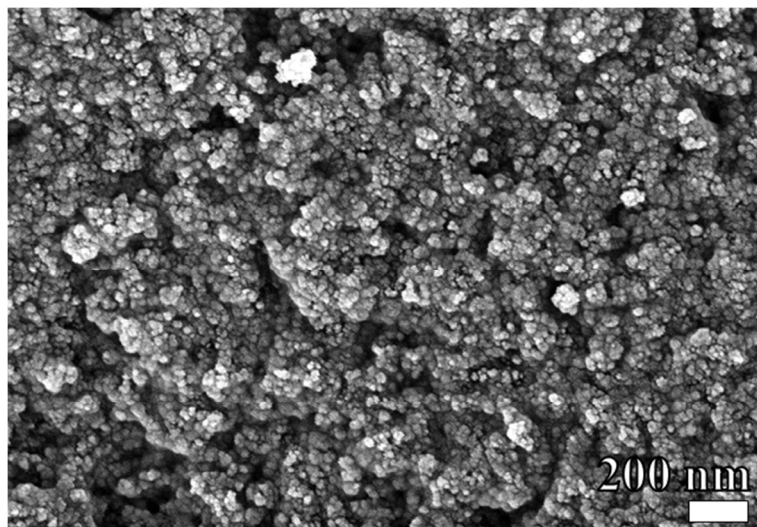


Figure S 1 SEM image of NDC support

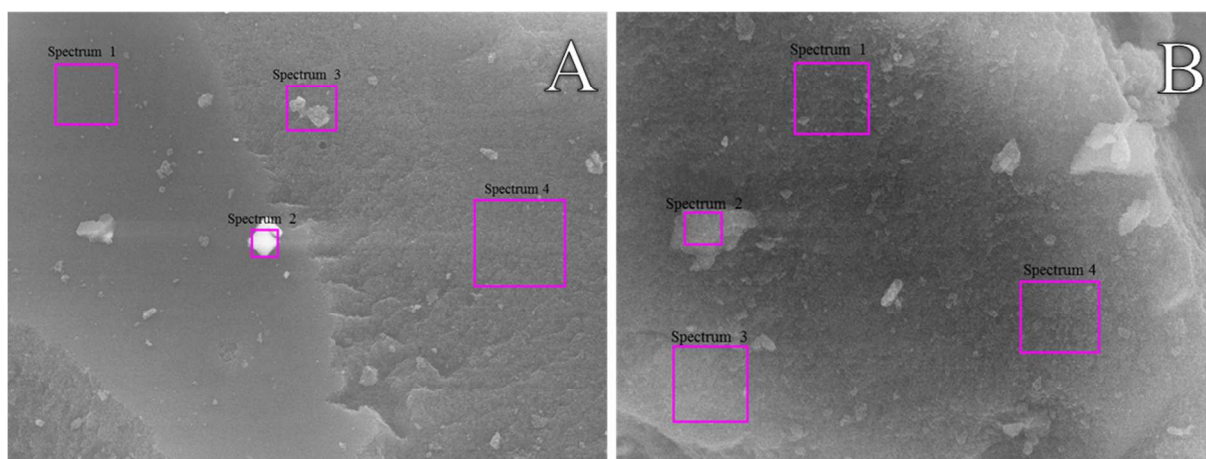


Figure S 2 EDX images of NDC support unwashed (A) and washed (B) from the iron impurities.

Table S 1 Elemental content in wt. % of Fe detected by SEM-EDX

Spectrum	Fe in unwashed NDC (wt. %)	Fe in washed NDC (wt. %)
1	15	0.8
2	51	0.6
3	12	0.9
4	10	0.6

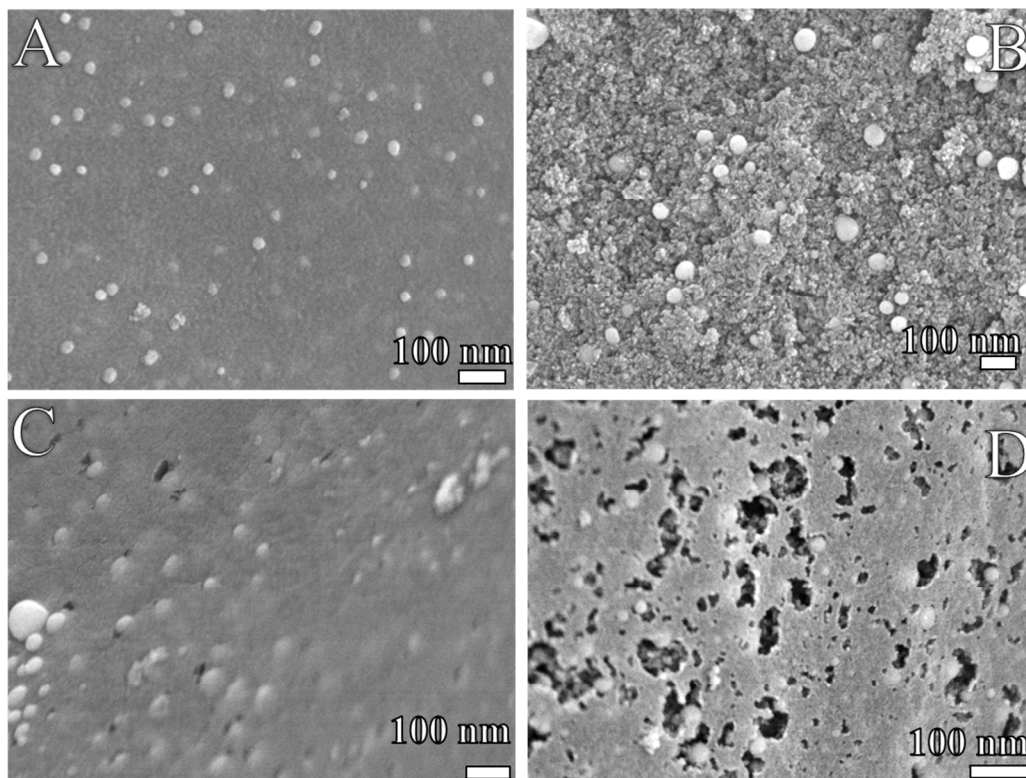


Figure S 3 These SEM images show the changes that occur to the Ni-NDC catalyst under different temperatures (A: 300 °C, B: 400 °C, C: 500 °C at which the high temperature effect starts, and D: 600 °C).

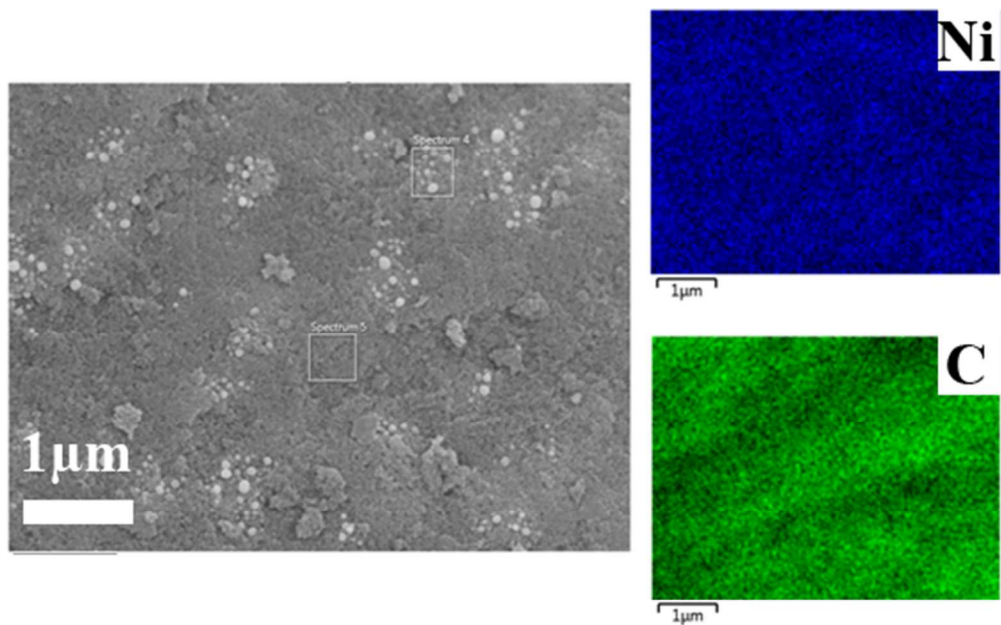


Figure S 4 SEM and EDX mapping on Ni-NDC composite

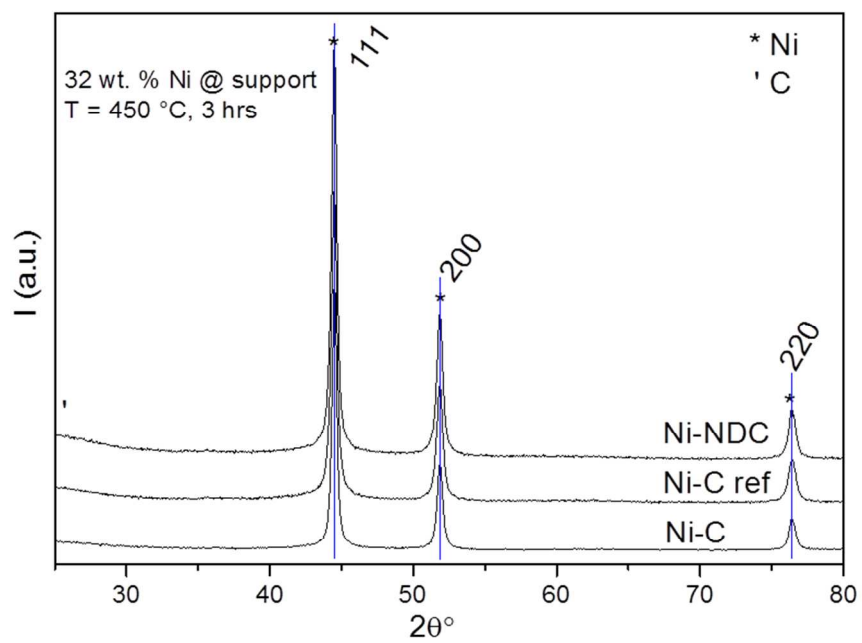


Figure S 5 XRD of Ni- composites before reactions

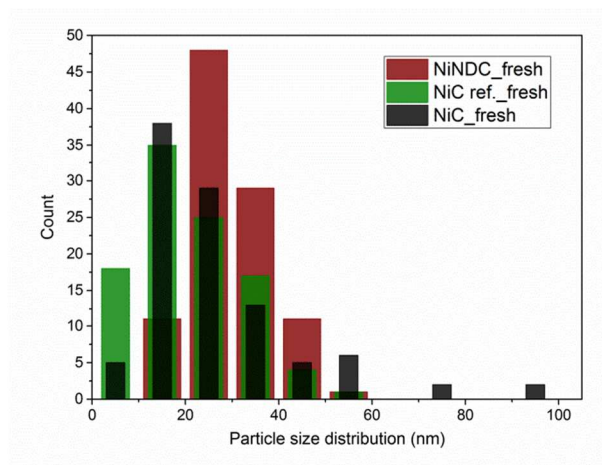
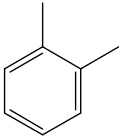
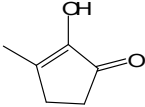
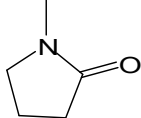
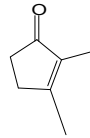
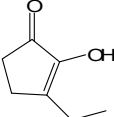
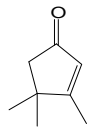
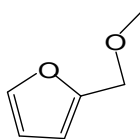
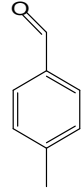
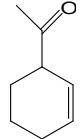
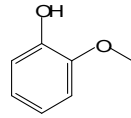


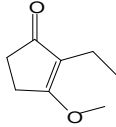
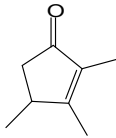
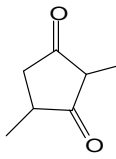
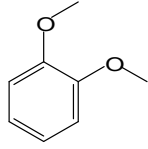
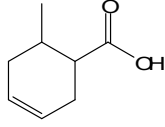
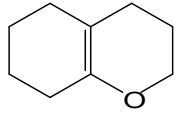
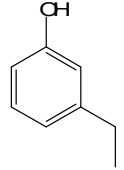
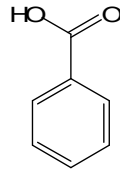
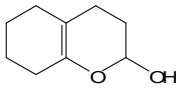
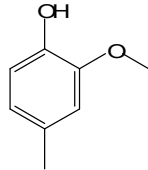
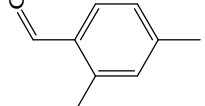
Figure S 6 Particle size distribution observed by several TEM images

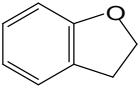
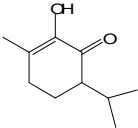
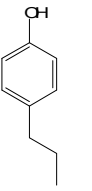
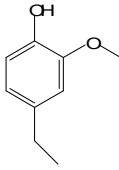
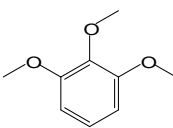
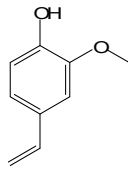
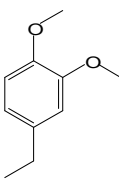
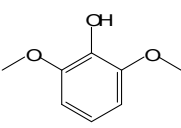
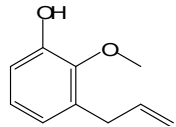
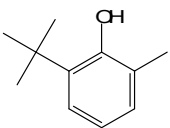
Table S 2 Several properties of the different fresh Ni-C composites

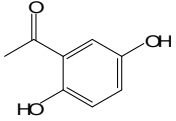
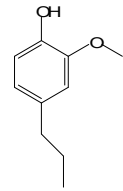
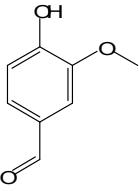
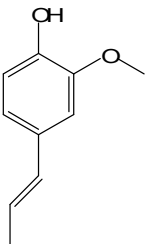
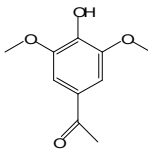
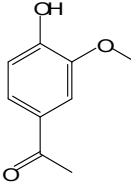
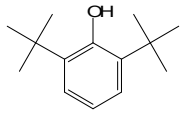
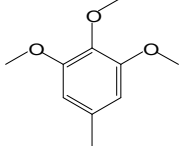
	SSA (m ² /g)	TPV (mL/g)	N (wt.%)	C (wt.%)	N/C ratio (wt.%)	Ni crystallite/particle size (nm)	
						XRD	TEM
NDC	790	1.34	3.20	80.0	0.040		
Ni- NDC	620	1.02	1.98	50.35	0.039	@ 76.42°	18.2
						@ 51.86°	17.0
						@ 44.49°	17.2
Cref	305	0.60	-	-	-		
Ni-Cref	155	0.79	-	71.16	-	@ 76.43°	15.4
						@ 51.85°	17.0
						@ 44.52°	17.3
C	980	1.13	-	-	-		
Ni-C	805	1.17	-	56.11	-	@ 76.43°	15.4
						@ 51.85°	16.3
						@ 44.48°	20.4

Table S 3 Compounds detected by GCxGC-MS in depolymerized lignin samples.

No.	Retention time	Mw	Compound
1.	13.085	106	
2.	18.197	112	
3.	18.209	99	
4.	18.646	110	
5.	19.393	126	
6.	19.543	124	
7.	19.995	112	
8.	20.112	120	
9.	20.444	124	
10.	20.446	124	

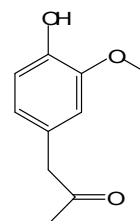
11.	20.891	140	
12.	21.190	138	
13.	21.345	126	
14.	22.097	138	
15.	22.392	140	
16.	22.541	138	
17.	22.993	122	
18.	22.996	122	
19.	23.593	154	
20.	23.745	138	
21.	24.296	134	

22.	24.496	120	
23.	25.091	168	
24.	25.694	136	
25.	26.295	152	
26.	27.049	168	
27.	27.197	150	
28.	27.345	166	
29.	27.953	154	
30.	28.545	164	
31.	28.692	164	

32.	28.697	152	
33.	28.844	166	
34.	29.158	152	
35.	30.797	164	
36.	31.397	196	
37.	31.555	166	
38.	32.591	206	
39.	32.599	182	

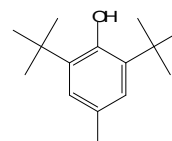
40. 32.605

180



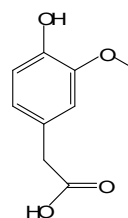
41. 32.740

220



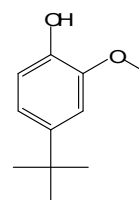
42. 33.051

182



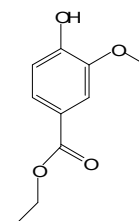
43. 33.498

180



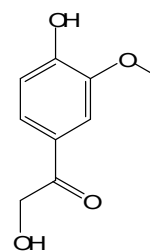
44. 33.952

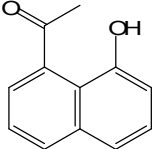
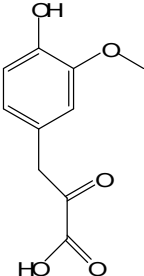
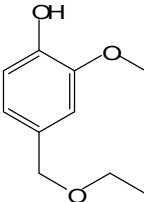
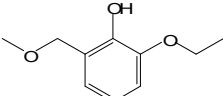
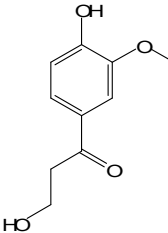
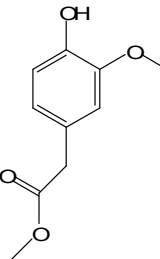
196

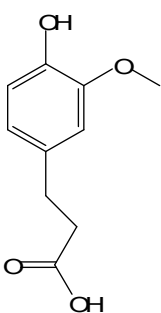
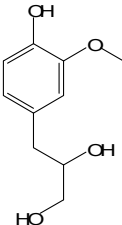
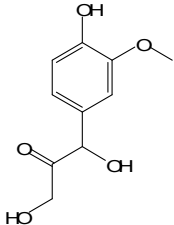
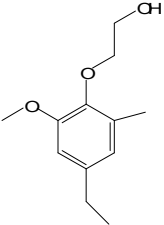
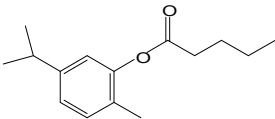
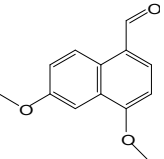


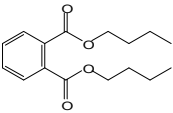
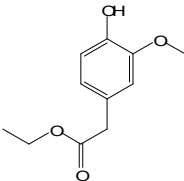
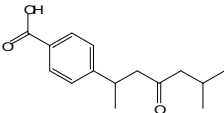
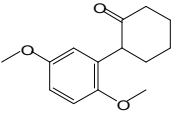
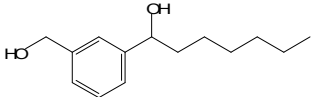
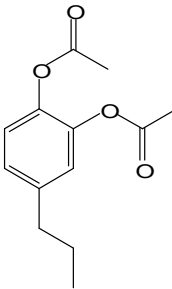
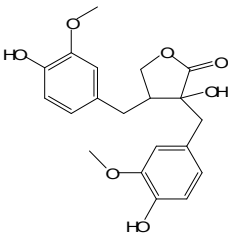
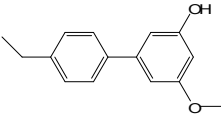
45. 33.954

182



46.	34.408	186	
47.	35.153	210	
48.	35.305	182	
49.	35.455	182	
50.	35.910	196	
51.	36.961	196	

52.	37.257	196	
53.	39.506	198	
52.	39.660	212	
54.	41.324	210	
55.	41.471	234	
56.	41.762	216	

57.	41.900	278	
58.	43.126	210	
59.	43.701	248	
60.	43.714	234	
61.	44.021	222	
62.	44.777	236	
63.	46.412	374	
64.	46.720	228	

65.

47.917

208

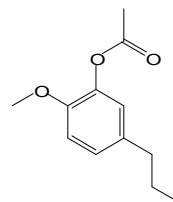


Figure 3 in the manuscript displays a two-dimensional gas chromatography (2D GC×GC-MS) image of the lignin bio-oil, obtained from hydrogenolysis of lignin in batch and flow systems in the presence of Ni-NDC catalyst. In the lignin bio-oil, the volatile components are mostly phenols, with 2 methoxy phenol derivatives as the dominant one, aside from a cyclopentene, benzene methoxy derivatives and bicyclic compounds as the major products. The 2D GC×GC image shows a greater number of products, which correspond to at least 85 wt% of the content vaporized in the GC injector at 300 °C.

Table S 4 ICP results of Ni content (mg/kg) in the products and the catalyst

	Sample	Ni, $\mu\text{g/g}$
Degraded lignin	Ni-C ref Batch	798
	Ni-C Batch	625
	Ni-C Flow	12
	Ni-NDC Batch	865
	Ni-NDC Flow	8.3
Catalyst	Fresh Catalyst	327750
	Ni-NDC Flow (after 100 hours)	273393
	Ni-NDC (after batch reaction)	110263

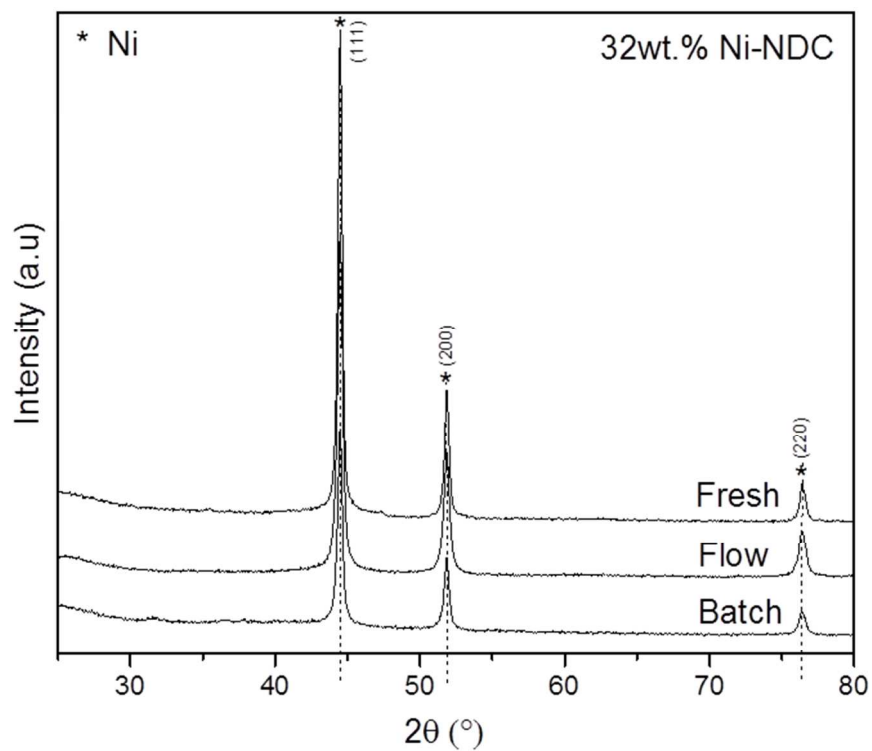


Figure S 7 XRD of Ni-NDC before reaction (Fresh), recovered from flow reaction of 100 hrs (Flow), and recovered from batch reaction of 24 hrs (Batch).

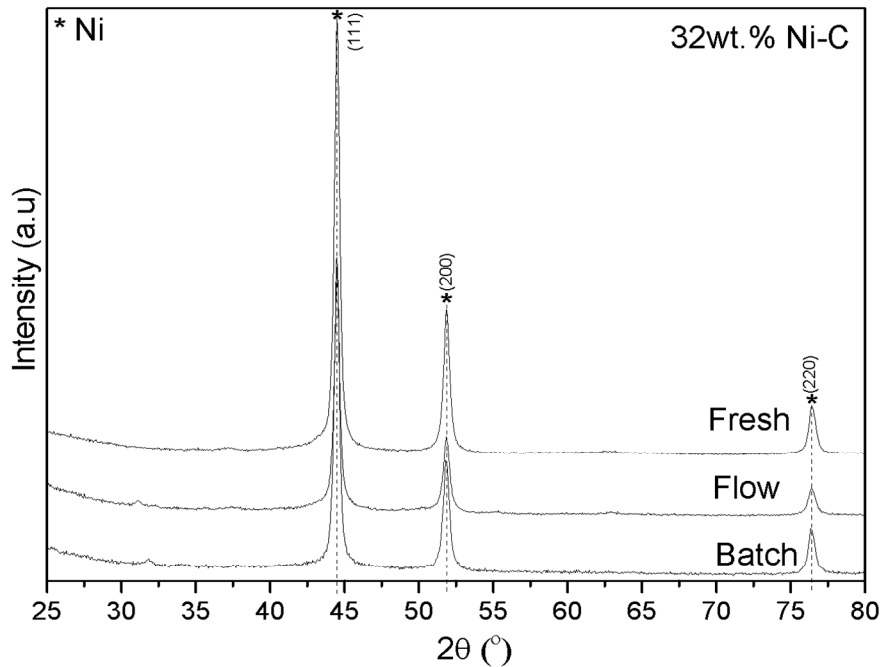


Figure S 8 XRD of Ni-C before reaction (Fresh), recovered from flow reaction of 25 hrs (Flow), and recovered from batch reaction of 24 hrs (Batch).

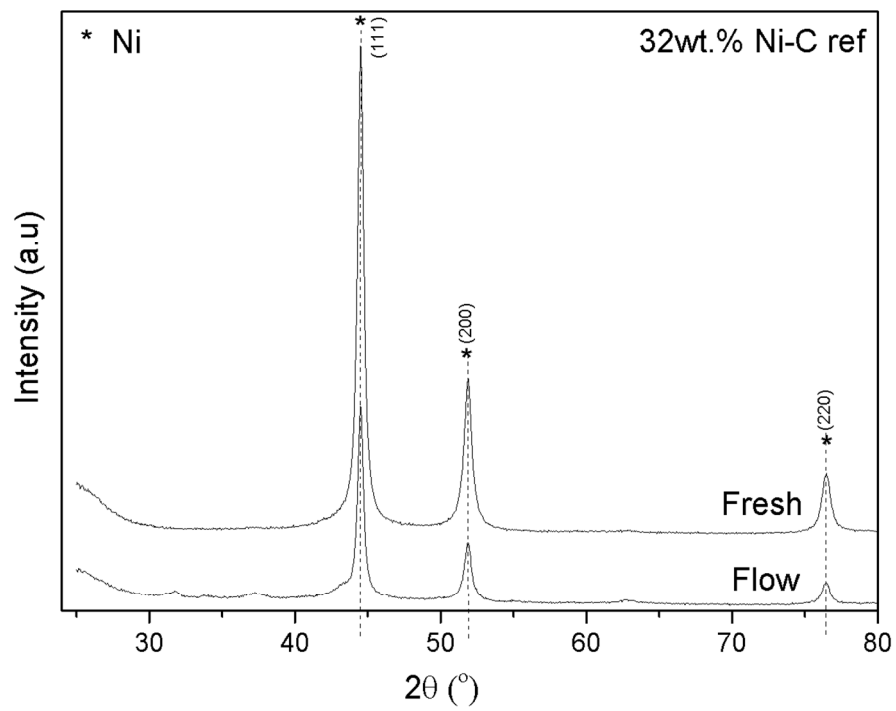


Figure S 9 XRD of Ni-C_{ref} before reaction (Fresh) and after being recovered from batch reaction of 24 hrs (Batch).

Table S 5 several properties of Ni-C composites after Flow and Batch reactions

	SSA (m ² /g)	TPV (mL/g)	N (wt.%)	C (wt.%)	Ni crystallite/particle size (nm)		Ni loss (Wt %)	Lignin mass balance (%)	
					XRD	TEM			
NDC-Ni flow (100 hours)	225	0.42	1.74	51.41	@76.50	18.2	20	5	99
					@51.85	16.9			
					@44.48	19.3			
NDC-Ni batch	13	0.05	1.08	53.71	@76.39	20.9	24	16	57
					@51.85	23.9			
					@44.49	26.4			
Ni-Cref flow	The porosity of this catalyst caused a high pressure and blockage when a flow of lignin solution was treated for degradation via catalytic hydrogenation system; therefore no flow reaction took place.								
Ni-Cref batch	27	0.056	0.27	59.08	@76.46	14.0	15	-	73
					@51.89	13.2			
					@44.50	14.9			
Ni-C flow (25hrs)	236	0.46	0.63	57.23	@76.40	16.2	38	-	99
					@51.84	18.8			
					@44.50	19.9			
Ni-C batch	62	0.17	0.78	56.32	@76.40	17.3	50	-	54
					@51.82	17.7			
					@44.50	19.9			

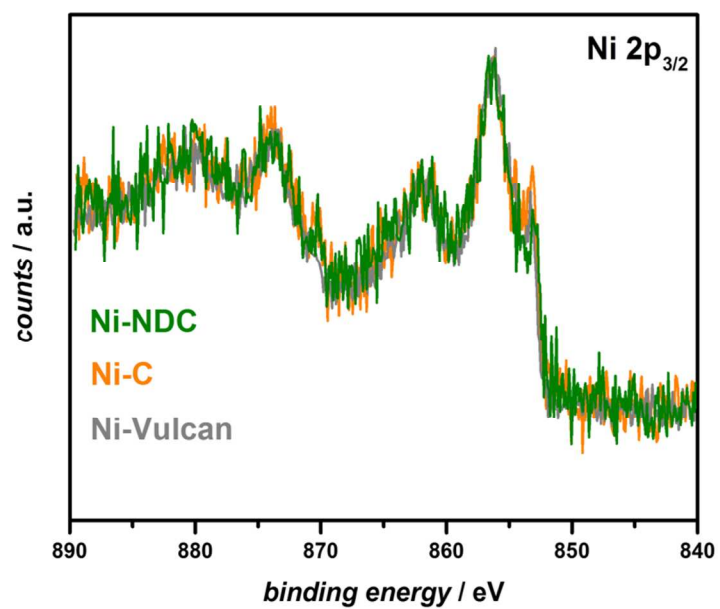


Figure S 10 X-ray photoelectron spectroscopy of Ni_{2p_{3/2}} bonds in the three catalytic systems (Ni-NDC, Ni-C and Ni-Vulcan).

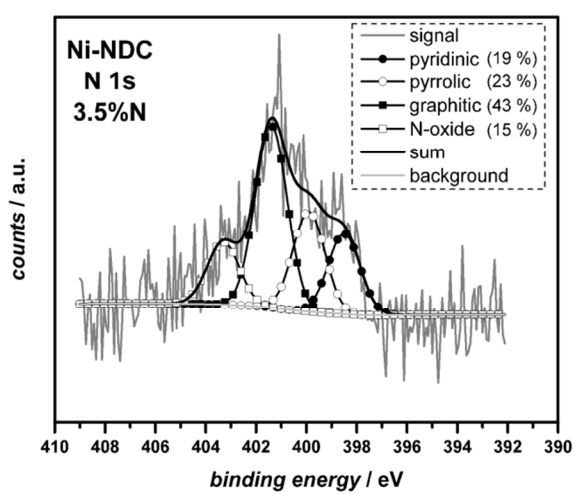
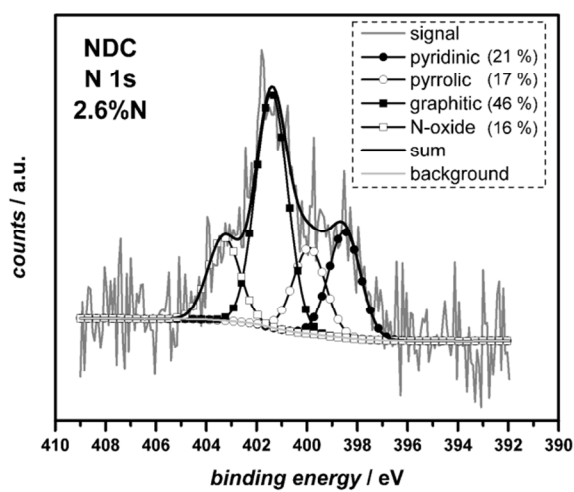
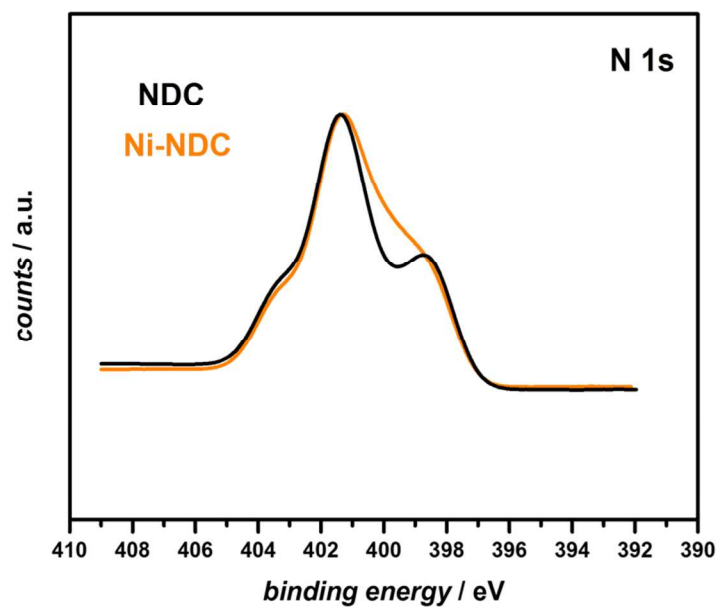


Figure S 11 X-ray photoelectron spectroscopy deconvolution curves of N_{1s} bonds in NDC and Ni-NDC

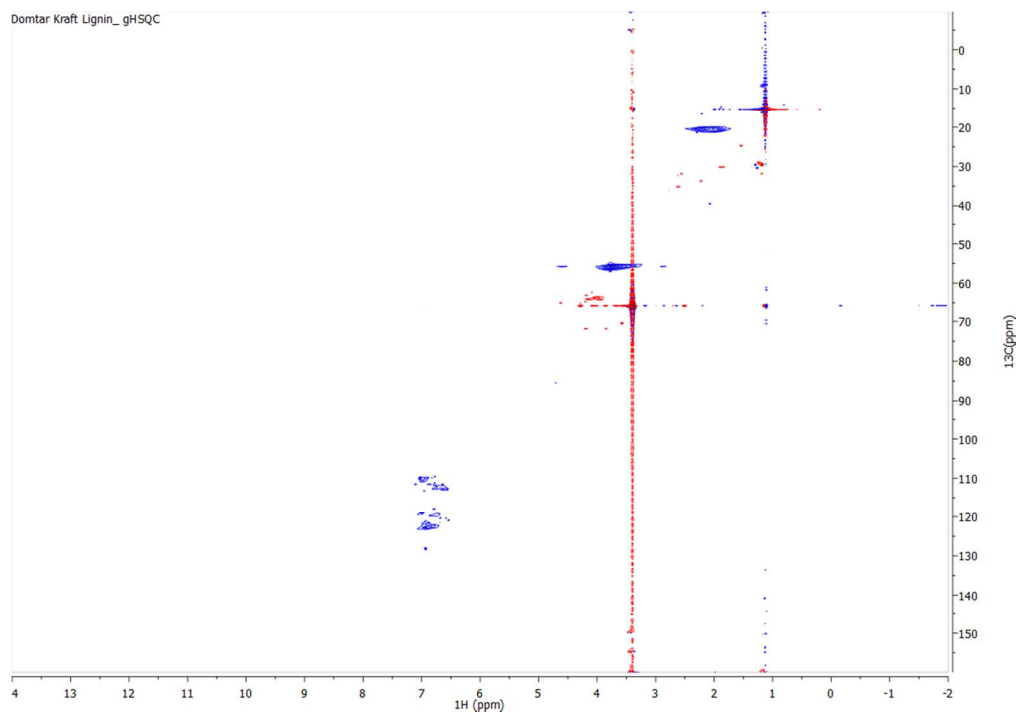


Figure S 12 2D-NMR of Kraft Lignin

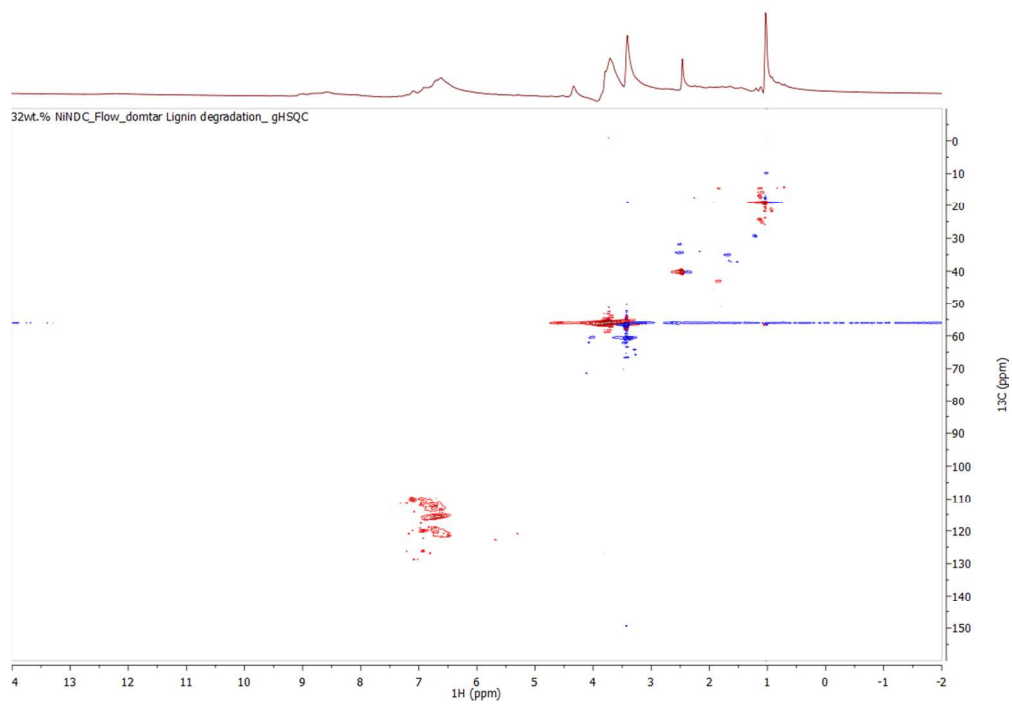


Figure S 13 2D-NMR of Kraft Lignin after flow reaction catalyzed by Ni-NDC

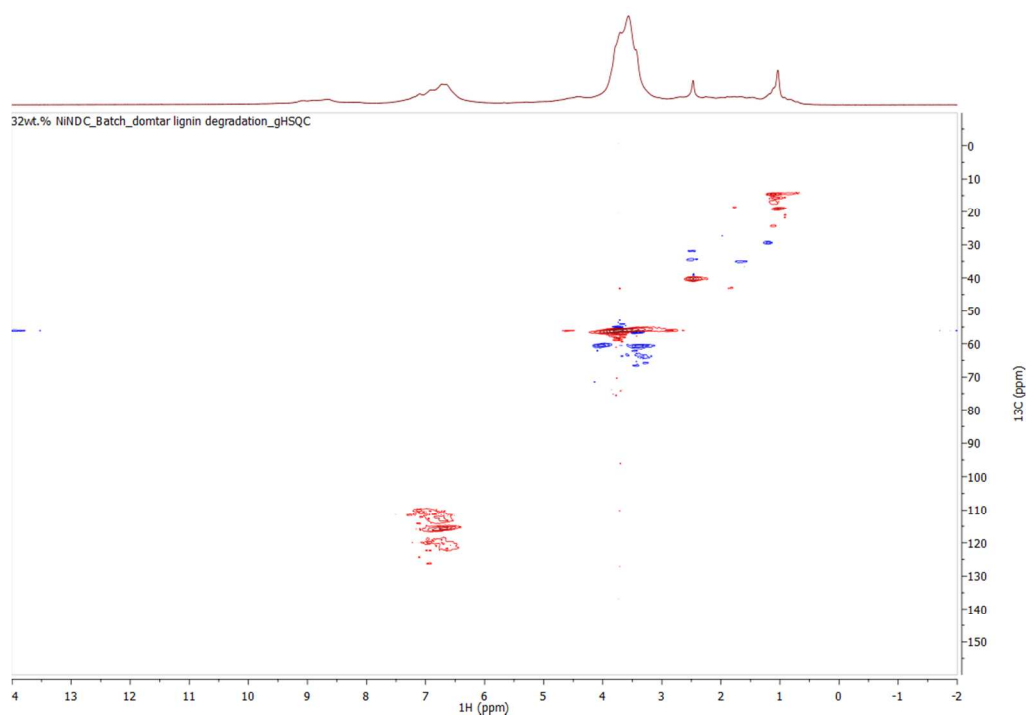


Figure S 14 2D-NMR of Kraft Lignin after batch reaction catalyzed by Ni-NDC

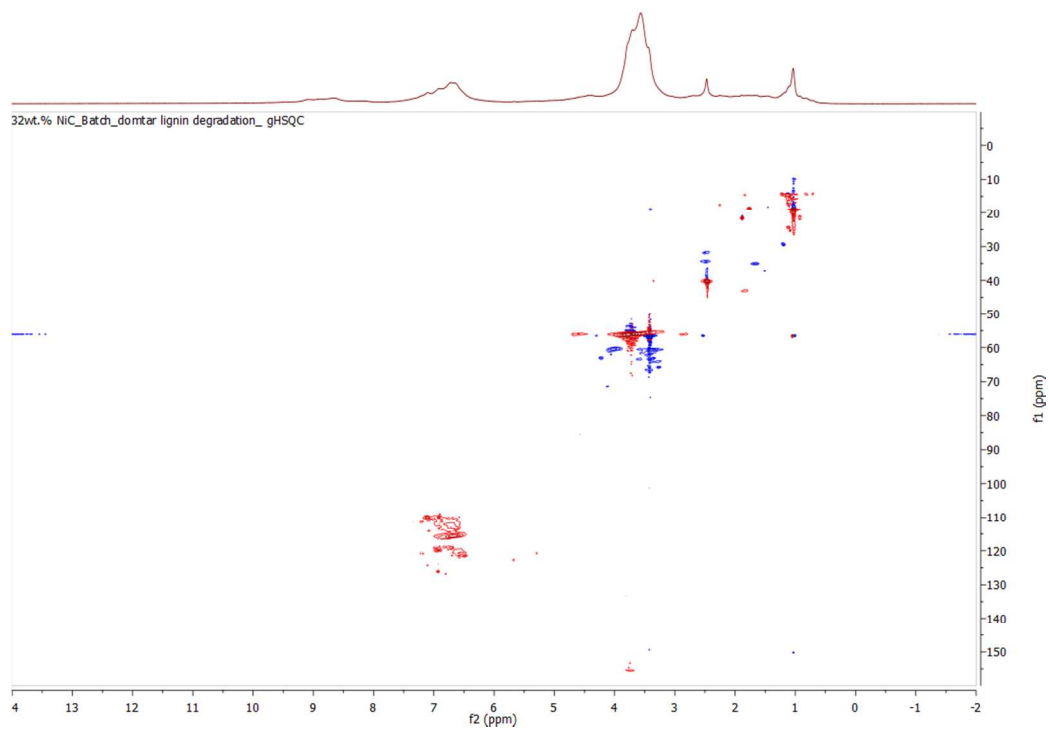


Figure S 15 2D-NMR of Kraft Lignin after batch reaction catalyzed by Ni-C

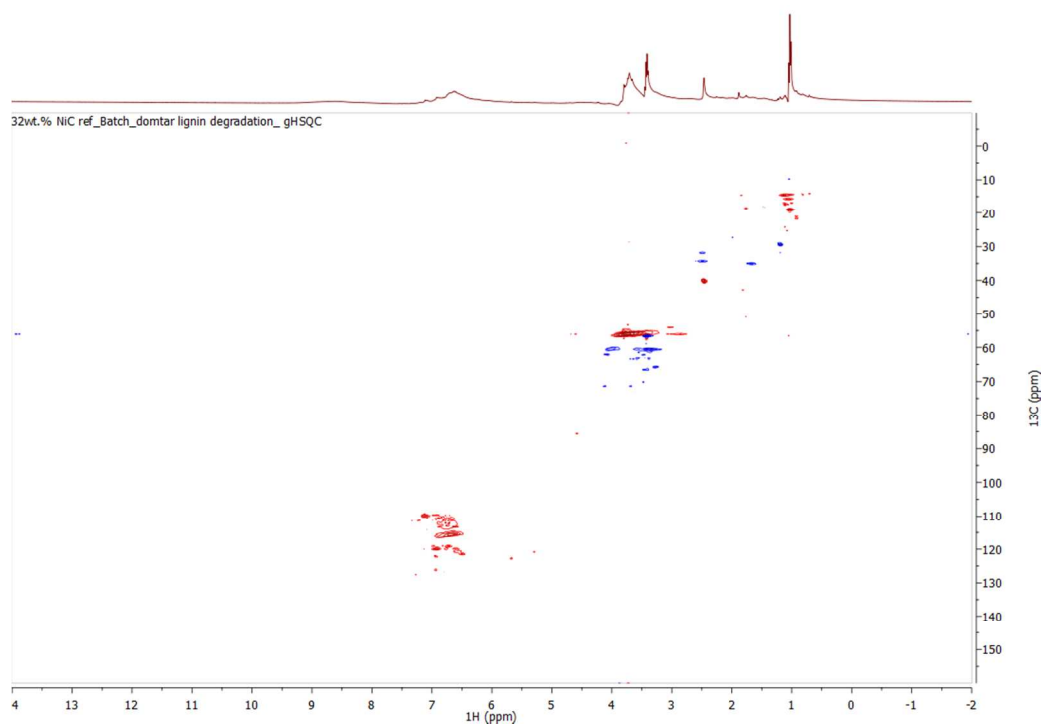


Figure S 16 2D-NMR of Kraft Lignin after batch reaction catalyzed by Ni-C_{ref}

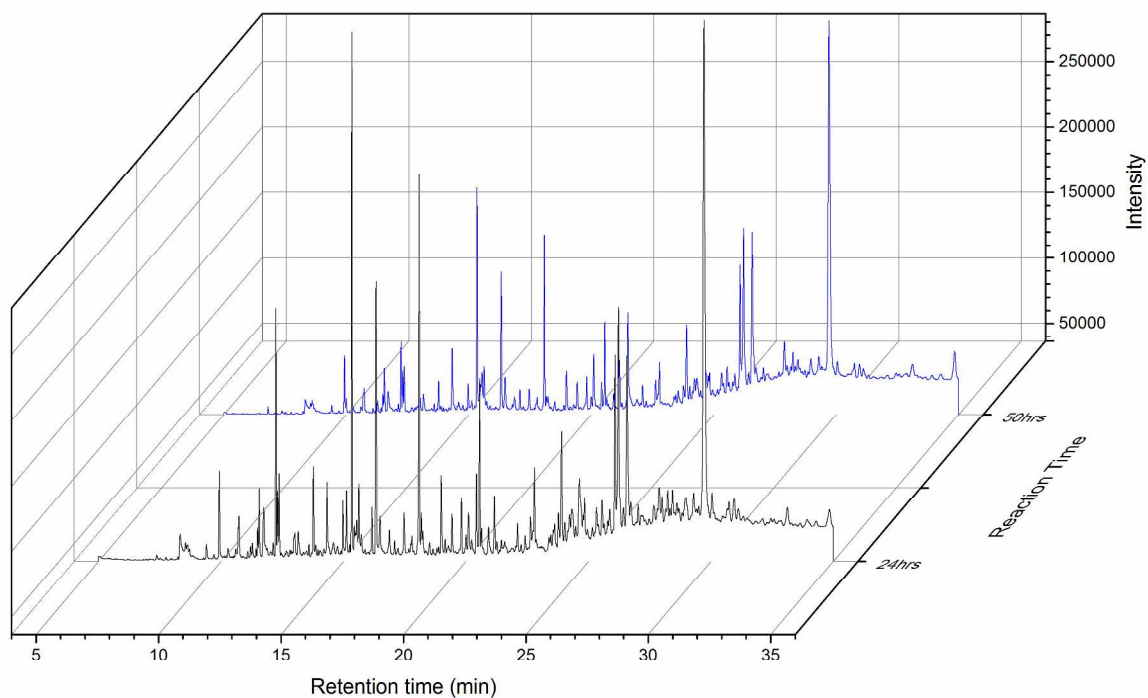


Figure S 17 GC-FID chromatograms of degraded lignin after 24 and 50 hours using Ni-NDC in the flow system

Table S 6 Elemental Analysis of the components of Ni-NDC under different reaction conditions

Sample	N (wt.%)	C (wt.%)	N/C ratio
NDC	3.2	80.0	0.040
Flow	1.7	50.7	0.033
Batch	0.9	49.5	0.020
Fresh NDC-Ni	1.8	48.6	0.038